OPEN ACCESS Freely available online

PLOS BIOLOGY

Tnfa Signaling Through Tnfr2 Protects Skin Against Oxidative Stress–Induced Inflammation

Sergio Candel[1,2☯], Sofía de Oliveira[1,2,3☯], Azucena López-Muñoz[1,2], Diana García-Moreno[1,2], Raquel Espín-Palazón[1,2], Sylwia D. Tyrkalska[1,2,4], María L. Cayuela[2,5], Stephen A. Renshaw[6], Raúl Corbalán-Vélez[7], Inmaculada Vidal-Abarca[8], Huai-Jen Tsai[9], José Meseguer[1,2], María P. Sepulcre[1,2], Victoriano Mulero[1,2]*

1 Departamento de Biología Celular e Histología, Facultad de Biología, Universidad de Murcia, Murcia, Spain, **2** Instituto Murciano de Investigación Biosanitaria (IMIB), Murcia, Spain, **3** Carlota Saldanha Lab, Instituto de Medicina Molecular, Instituto de Bioquímica, Faculdade de Medicina, Universidade de Lisboa, Lisboa, Portugal, **4** Instituto de Investigaciones Marinas, Consejo Superior de Investigaciones Científicas (CSIC), Vigo, Spain, **5** Grupo de Telómeros, Envejecimiento y Cáncer, Unidad de Investigación, Departamento de Cirugía, CIBERehd. Hospital Universitario "Virgen de la Arrixaca," Murcia, Spain, **6** MRC Centre for Developmental and Biomedical Genetics, University of Sheffield, Sheffield, United Kingdom, **7** Servicio de Dermatología, Hospital Universitario "Virgen de la Arrixaca," Murcia, Spain, **8** Servicio de Anatomía Patológica, Hospital Universitario "Virgen de la Arrixaca," Murcia, Spain, **9** Institute of Molecular and Cellular Biology, National Taiwan University, Taipei, Taiwan

Abstract

TNFα overexpression has been associated with several chronic inflammatory diseases, including psoriasis, lichen planus, rheumatoid arthritis, and inflammatory bowel disease. Paradoxically, numerous studies have reported new-onset psoriasis and lichen planus following TNFα antagonist therapy. Here, we show that genetic inhibition of Tnfa and Tnfr2 in zebrafish results in the mobilization of neutrophils to the skin. Using combinations of fluorescent reporter transgenes, fluorescence microscopy, and flow cytometry, we identified the local production of dual oxidase 1 (Duox1)-derived H_2O_2 by Tnfa- and Tnfr2-deficient keratinocytes as a trigger for the activation of the master inflammation transcription factor NF-κB, which then promotes the induction of genes encoding pro-inflammatory molecules. In addition, pharmacological inhibition of Duox1 completely abrogated skin inflammation, placing Duox1-derived H_2O_2 upstream of this positive feedback inflammatory loop. Strikingly, DUOX1 was drastically induced in the skin lesions of psoriasis and lichen planus patients. These results reveal a crucial role for TNFα/TNFR2 axis in the protection of the skin against DUOX1-mediated oxidative stress and could establish new therapeutic targets for skin inflammatory disorders.

Citation: Candel S, de Oliveira S, López-Muñoz A, García-Moreno D, Espín-Palazón R, et al. (2014) Tnfa Signaling Through Tnfr2 Protects Skin Against Oxidative Stress–Induced Inflammation. PLoS Biol 12(5): e1001855. doi:10.1371/journal.pbio.1001855

Academic Editor: Douglas R. Green, St. Jude Children's Research Hospital, United States of America

Received November 8, 2013; **Accepted** March 28, 2014; **Published** May 6, 2014

Funding: This work was supported by the Spanish Ministry of Science and Innovation (grants BIO2011-23400 and CSD2007-00002 to VM, and PhD fellowship to SC, all co-funded with Fondos Europeos de Desarrollo Regional/European Regional Development Funds), the Fundación Séneca-Murcia (grant 04538/GERM/06 to VM and PhD fellowship to RE-P), Fundação para a Ciência e Tecnologia (PhD fellowship to SdO, SFRH/BD/62674/2009), a Medical Research Council Senior Clinical fellowship to SAR (G0701932), and the European 7th Framework Initial Training Network FishForPharma (PhD fellowship to SDT, PITG-GA-2011-289209). The funders had no role in study design, data collection and analysis, decision to publish, or preparation of the manuscript.

Competing Interests: The authors have declared that no competing interests exist.

* E-mail: vmulero@um.es

☯ These authors contributed equally to this work.

Abbreviations: CHT, caudal hematopoietic tissue; DN, dominant negative; Duox, dual oxidase; HIF, hypoxia-inducible factor; H&E, haematoxylin and eosin; IBD, inflammatory bowel disease; Il1b, interleukin-1β; IP, incontinentia pigmenti; MO, morpholino; PFA, paraformaldehyde; Ptgs2, prostaglandin-endoperoxide synthase 2; ROS, reactive oxygen species; Tnf, tumor necrosis factor, Tnfr, Tnf receptor.

Introduction

Tumor necrosis factor α (TNFα) is a multifunctional cytokine that mediates key roles in acute and chronic inflammation, antitumor responses, and infection. TNFα binds TNF receptor 1 (TNFR1, also known as TNFRSF1A or P55) and TNFR2 (also known as TNFRSF1B or P75) for stimulation of two opposing signaling events [1]. In general, TNFR1 signaling results in the trigger of a cascade that can result in apoptosis [2]. This is dependent upon the cell type, the state of activation of the cell, and the cell cycle. In contrast, a TNFR2 signal induces cell survival pathways that can result in cell proliferation [2].

Enhanced TNFα synthesis is associated with the development of autoimmune/chronic inflammatory diseases, including psoriasis, lichen planus, rheumatoid arthritis, and inflammatory bowel disease (IBD). The inhibition of TNFα activities in these diseases has been remarkably successful [3,4]. Paradoxically, however, numerous studies have reported new-onset psoriasis and lichen planus, or worsening of existing psoriasis, following TNFα antagonist therapy in adult patients [5–10]. Despite these clinical data pointing to an ambiguous function of TNFα in psoriasis and lichen planus, the role of TNFα, and in particular the contribution of each TNFR, in the regulation of skin inflammation has been scarcely studied. An earlier study using gene-targeted mutant mice lacking either TNFR1 or TNFR2 showed that skin inflammation induced indirectly by irritant chemicals or directly by intradermal administration of TNFα was greatly attenuated in TNFR1-deficient mice, whereas TNFR2-deficient siblings responded normally [11]. In addition, mice with an arrested canonical NF-κB activation pathway in the keratinocytes develop a severe

Author Summary

Psoriasis and lichen planus are chronic, debilitating skin diseases that affect millions of people worldwide. TNFα is a multifunctional cytokine that mediates acute and chronic inflammation. While TNFα antagonist therapy is used for autoimmune or chronic inflammatory diseases, such as inflammatory bowel disease (IBD), numerous studies have reported new-onset psoriasis and lichen planus following such therapy. We have used the unique advantages of the zebrafish embryo to identify a novel phenotype that mirrors this unexplained and paradoxical onset of psoriasis and lichen planus. We found that depletion of Tnfa or its receptor Tnfr2 caused skin inflammation and hyperproliferation of keratinocytes through the activation of a Duox1/H_2O_2/NF-κB positive feedback inflammatory loop. Strikingly, DUOX1 was drastically induced in the skin lesions of psoriasis and lichen planus patients, and pharmacological inhibition of Duox1 abrogated skin inflammation, placing Duox1-derived H_2O_2 upstream of this inflammatory loop. Our results suggest that therapies targeting DUOX1 and H_2O_2 could provide innovative approaches to the management of skin inflammatory disorders.

inflammatory skin disease shortly after birth, which is caused by TNFα- and macrophage-mediated, but T-cell–independent, mechanisms [12–16]. The characteristics of this complex disorder are strikingly similar to those associated with the human X-linked genodermatosis incontinentia pigmenti (IP) [17]. To the best of our knowledge, however, the role played by TNFα in the homeostasis of healthy skin has never been studied.

TNFα and TNFRs are conserved in all vertebrates. Recent studies have shown that in the zebrafish (*Danio rerio*) Tnfa functions as a pro-inflammatory cytokine [18] and Tnfr signaling plays an important role in the homeostasis of endothelial cells [19]. In the present study, we have taken advantage of the strengths of the zebrafish embryo model to study the impact of Tnfa, Tnfr1, and Tnfr2 deficiencies in a whole vertebrate organism. We found that Tnfa and Tnfr2 are both crucial, whereas Tnfr1 is dispensable, for the homeostasis of the skin. Genetic inhibition of Tnfa and Tnfr2 promotes H_2O_2-mediated skin infiltration by neutrophils, increased keratinocyte proliferation, and the local activation of the master inflammation transcription factor NF-κB, which then promotes the induction of genes encoding pro-inflammatory molecules. In addition, DUOX1 was strongly induced in keratinocytes of human psoriasis and lichen planus patients.

Results

Tnfa or Tnfr2 Deficiency Results in Neutrophil Mobilization to the Skin

In wild-type larvae, most neutrophils (approximately 90%) were located in the caudal hematopoietic tissue (CHT) [20] by 3 d postfertilization (dpf) (Figure 1A–C), which is consistent with neutrophil localization patterns described previously [21,22]. However, in Tnfa- and Tnfr2-deficient larvae, approximately 40% of neutrophils were located outside the CHT (Figure 1A–C). In addition, Tnfr1-deficient animals showed a normal neutrophil distribution, whereas their double deficient siblings for both Tnfr1 and Tnfr2 showed also a distribution pattern more similar to single Tnfr2-deficient fish (Figure 1A–C). The specificity of this phenotype was confirmed with a dominant negative (DN) Tnfr2, which is lacking the entire intracellular signaling domain, but is identical to full-length Tnfr2 in its transmembrane and extracellular domains, and therefore, its trimerization with endogenous Tnfr2 extinguishes Tnfr2 signaling [19]. The results showed that the altered neutrophil distribution of Tnfr2 morphants was phenocopied by overexpression of DN-Tnfr2 (Figure S1A). In addition, the scattered distribution of Tnfa- and Tnfr2-deficient larvae was partially rescued by overexpression of wild-type Tnfa and Tnfr2 RNAs, respectively (Figure S1B). These results prompted us to examine the distribution of macrophages in TNFα- and TNFR2-deficient fish, and surprisingly, macrophage distribution was apparently normal in all cases (Figure S2).

To ascertain the precise localization of neutrophils in Tnfa/Tnfr2-deficient larvae, we knocked down Tnfr2 in transgenic *mpx:eGFP* animals followed by whole mount immunohistochemistry (WIHC) against p63 (basal keratinocyte marker) to visualize neutrophils (GFP^+) and skin keratinocytes ($p63^+$) at the same time in whole larvae. The results revealed that although neutrophils from wild-type animals were mainly located in the CHT, a high proportion of neutrophils were seen in close contact with keratinocytes in Tnfr2-deficient animals (Figure 1D and Videos S1 and S2). Collectively, these results indicate that deficiency of either Tnfa or Tnfr2 specifically promotes neutrophil infiltration into the skin of zebrafish during early development.

Tnfa or Tnfr2 Deficiency Triggers the Induction of Genes Encoding Pro-Inflammatory Mediators in Keratinocytes

The phenotype of Tnfa- and Tnfr2-deficient fish is reminiscent of that of *spint1a* and *clint1* mutant fish, which show chronic skin inflammation characterized by increased interleukin-1β (IL-1β) production and neutrophil infiltration [23–25]. This led us to examine the expression of three genes encoding major pro-inflammatory molecules, namely Tnfa itself, IL-1β, and prostaglandin-endoperoxide synthase 2b (PTGS2b, also known as COX2b), in whole wild-type and Tnfr2-deficient larvae at 3 dpf as well as in sorted *mpx:eGFP*$^+$ cells—that is, neutrophils. It was found that Tnfr2 deficiency triggered the expression of *tnfa*, *il1b*, and *ptgs2b* genes (Figure 2A). Although neutrophils highly expressed the genes encoding Tnfa and Il1b as well as both Tnfrs, they did not mediate the induction of *il1b* observed in Tnfr2-deficient fish (Figures 2B, S3A, and S4A). Nevertheless, the transcript levels of *tnfa* were higher in neutrophils from Tnfr2-deficient fish than in neutrophils from their wild-type siblings (Figure 2B), but this might reflect a positive feedback loop in response to Tnfr2 deficiency [19]. In addition, Tnfr2-deficient embryos showed higher transcript levels of *il1b* at 24 hpf (Figure S5), soon after the development of the first neutrophils in the zebrafish embryo [21,22,26] and before hatching. We then sorted $krt18^+$ cells from Tnfa- and Tnfr2-deficient animals at 3 dpf and found that they show much higher transcript levels of *il1b* and *ptgs2b* than $krt18^+$ cells from wild-type animals (Figures 2C and S3B). Notably, $krt18^+$ cells expressed both Tnf receptors (Figure S4B) and the specific marker of basal keratinocytes p63 (Figure S3B).

We next wondered whether knockdown of Il1b using a specific morpholino (MO) [27] might rescue the neutrophil dispersion of Tnfr2-deficient animals. As shown in Figure 2D, genetic inhibition of Il1b failed to rescue the neutrophil dispersion observed in Tnfr2 morphants. These results taken together indicate that the Tnfa/Tnfr2 axis is required for skin homeostasis in zebrafish and that the deficiency of either ligand or receptor triggers an inflammatory response characterized by the induction of pro-inflammatory mediators and neutrophil infiltration.

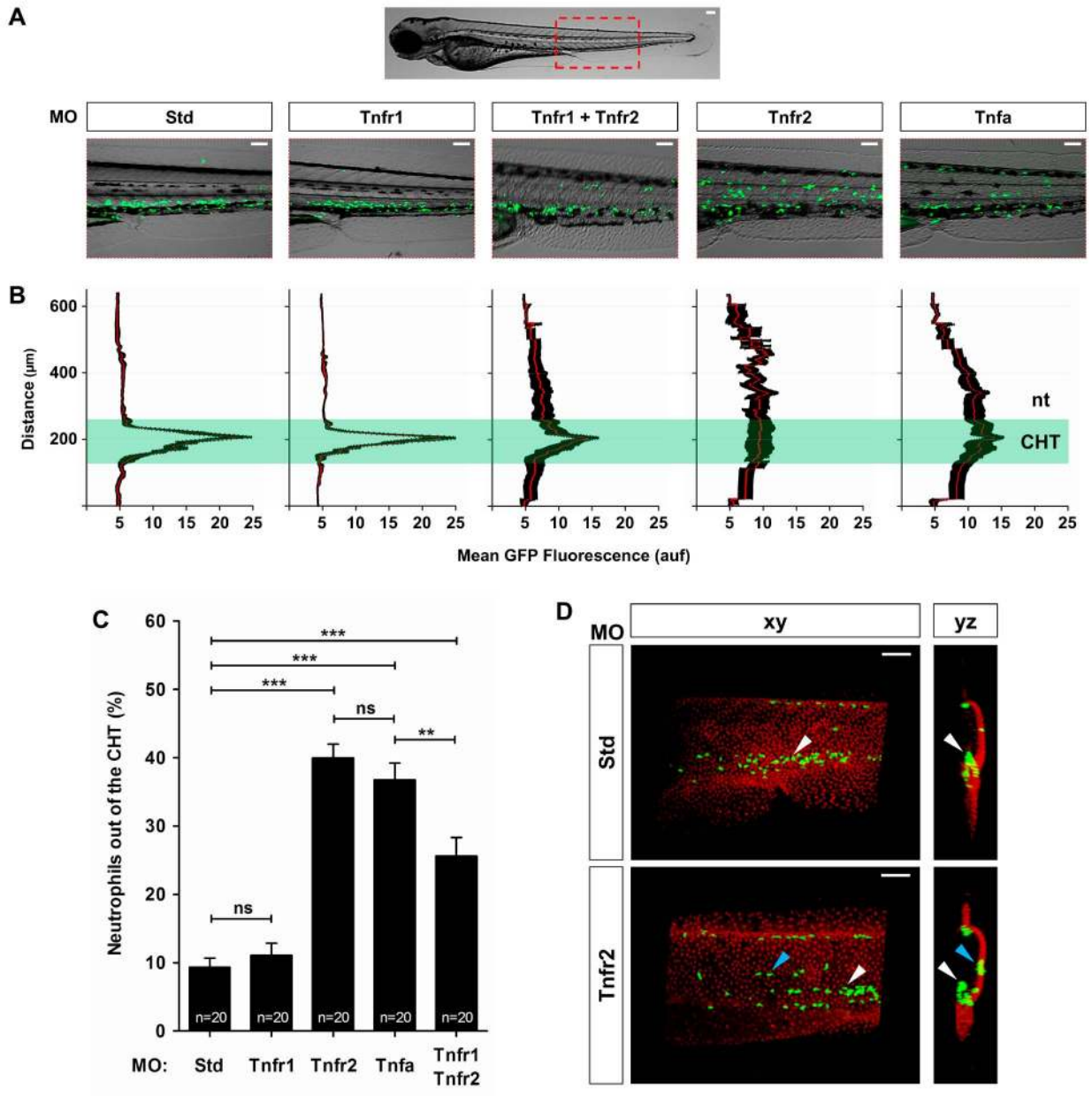

Figure 1. TNFα and Tnfr2 deficiencies result in neutrophil mobilization to the skin. Zebrafish one-cell *mpx:eGFP* and/or *krt18:RFP* embryos were injected with standard control (Std), Tnfr1, Tnfr2, Tnfa, or Tnfr1+Tnfr2 MOs. (A) Representative images, bright field and green channels, of the morphants at 3 dpf showing the differences in the neutrophils distribution. (B) Fluorescence intensity was measured for all the groups in the area indicated (A), which includes the CHT, where most neutrophils are located in wild-type larvae at 3 dpf. The images were converted to a fluorescence value matrix where the value obtained for each pixel transversally was the mean ± S.E.M. for all the pixels for each row (15 larvae per treatment from 3 different experiments). The area corresponding to the CHT has been labeled and highlighted. The notochord (nt) location has been indicated to facilitate the larval orientation. auf, arbitrary units of fluorescence. (C) The neutrophil mobilization from the CHT in Tnfa- and Tnfr2-deficient larvae was quantified as the percentage of neutrophils outside the CHT in 20 larvae per group from 3 different experiments. The mean ± S.E.M. for each group is shown. (D) Representative frontal (*xy*) and lateral (*yz*) views of tridimensional reconstructions from confocal microscopy images of WIHC of *mpx:eGFP* larvae stained at 3 dpf with anti-p63 antibodies (basal keratinocyte marker, red) showing the neutrophils' distribution in the CHT area of control and Tnfr2-deficient larvae. Note that most neutrophils (eGFP, green) are located in the CHT in control larvae (white arrowheads), while many of them infiltrate the skin (blue arrowheads) of Tnfr2-deficient larvae, whereas they are mainly located in the CHT in their wild-type siblings. Scale bars, 100 µm. ns, not significant. *$p<0.05$, **$p<0.01$, ***$p<0.001$.
doi:10.1371/journal.pbio.1001855.g001

Tnfa and Tnfr2 Deficiencies Induce NF-κB Activation in the Skin

The master regulator of inflammation NF-κB plays an essential role in the homeostasis of skin. Thus, genetic inhibition of the NF-κB pathway in keratinocytes triggers a severe inflammatory skin disease in newborn mice, which is completely rescued by Tnfa and Tnfr1 depletion [12–16]. We therefore use a NF-κB reporter line [28] to visualize the dynamics of NF-κB in whole Tnfr2-deficient larvae. Injection of bacterial DNA, which activated TLR9, resulted in a drastic activation of NF-κB in the whole larvae

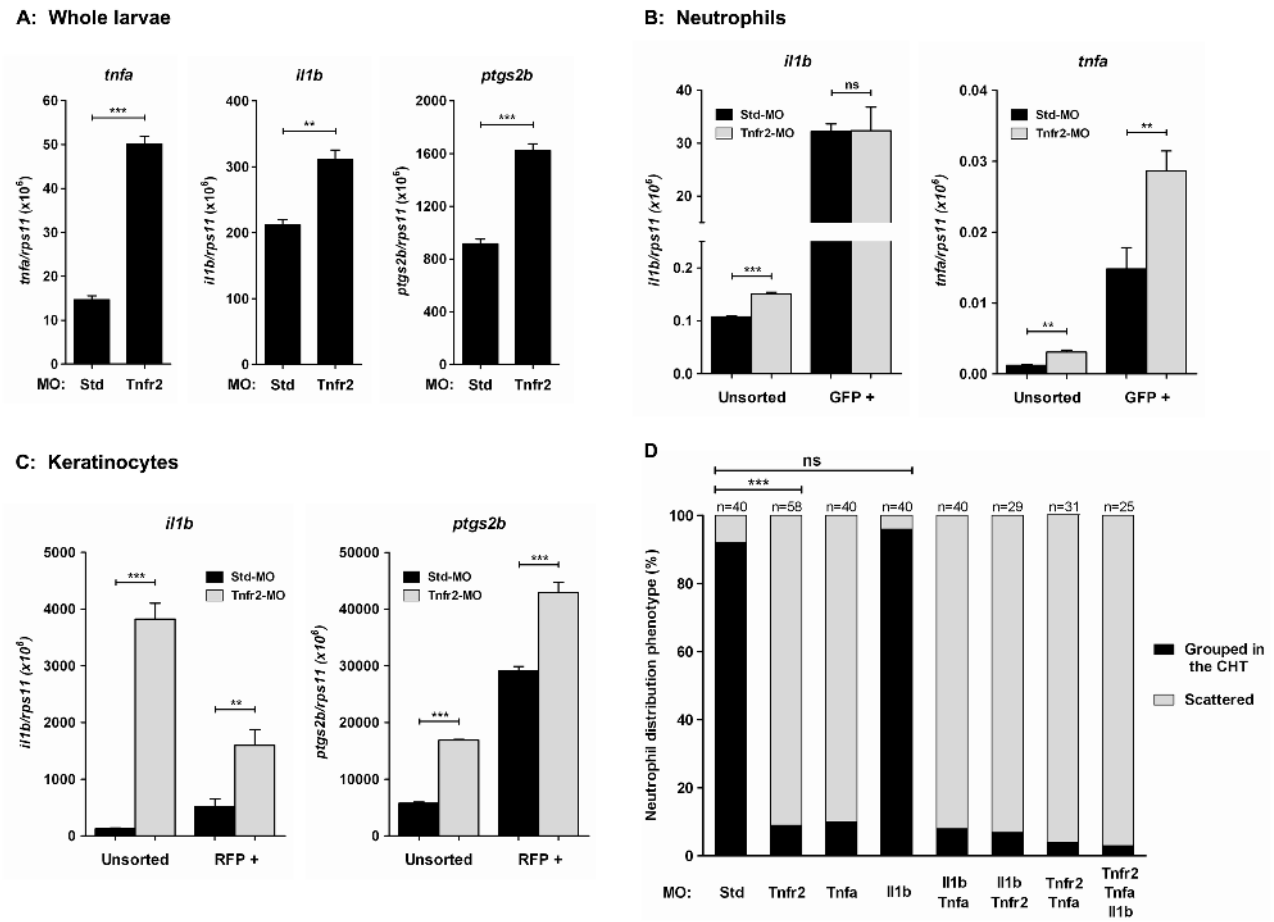

Figure 2. TNFa and Tnfr2 deficiencies trigger skin inflammation. Zebrafish one-cell *mpx:eGFP* or *krt18:RFP* embryos were injected with standard control (Std), Tnfr2, Il1b, and/or Tnfa MOs. The expression of *tnfa*, *il1b*, and *ptgs2b* genes was measured by RT-qPCR in whole body (A), FACS-sorted neutrophils (B), and FACS-sorted keratinocytes (C) from Std and Tnfr2 morphants at 3 dpf. (D) The phenotype of 3 dpf morphant larvae was classified as neutrophils grouped in the CHT or scattered, as described in Figure 1. Note that IL-1β knockdown failed to rescue the neutrophil mobilization in Tnfr2-deficient larvae. ns, not significant. *$p<0.05$; **$p<0.01$; ***$p<0.001$.
doi:10.1371/journal.pbio.1001855.g002

(Figure 3A–B), as expected from previous results [29,30]. Interestingly, Tnfr2 deficiency promoted a restricted activation of NF-κB in the skin (Figure 3A–E and Videos S3 and S4). Furthermore, although skin integrity was unaffected up to 5 dpf in Tnfr2-deficient larvae, as assayed by histology (Figure S6), they showed increased keratinocyte proliferation, as assayed in double transgenic NF-κB:eGFP; *krt18:RFP* animals and double WIHC with anti-RFP and anti-phosphorylated H3 (Figure 4).

Tnfa and Tnfr2 Deficiencies Trigger H_2O_2 Production in the Skin

Hydrogen peroxide gradients were recently shown to contribute to the early influx of neutrophils in wound [31] and tumor [32]. Interestingly, however, H_2O_2 is not required for neutrophil detection of localized infection [33]. These gradients are created by the dual oxidase 1 (Duox1) [31] and sensed by neutrophils through the tyrosine kinase Lyn [34]. Although identified and best studied in the zebrafish, H_2O_2 is likely to play the same function in human neutrophils [34]. We first analyzed the expression of the gene encoding Duox1 and found that Tnfr2-deficient keratinocytes showed higher transcript levels of *duox1* than wild-type animals (Figure 5A). Next, using an H_2O_2-detecting fluorescence probe, we observed that Tnfr2-deficient larvae also produced H_2O_2 in the skin (Figure 5B,C). We observed similar levels of labeling with the H_2O_2 probe in Tnfr2-deficient keratinocytes and in local keratinocytes after wounding (Figure S7). Notably, H_2O_2 production by Tnfr2-deficient keratinocytes preceded the activation of NF-κB (Figure S8). Consistent with these observations, genetic inhibition of Duox1 with a specific MO [31] was able to partially prevent the infiltration of neutrophils into the skin of Tnfr2-deficient larvae (Figure 5D,E). To further confirm this result, we designed a DN form of Duox1 [35], and notably, overexpression of DN-Duox1 was also able to partially prevent neutrophil infiltration in Tnfr2-deficient larvae (Figure S9A,B). Furthermore, we knocked down the H_2O_2 sensor of neutrophils, Lyn [34], and found full prevention of neutrophil infiltration in both Tnfr2- and Tnfa-deficient animals (Figure 5F,G).

Pharmacological Inhibition of Duox1 Restores Skin Homeostasis in Tnfa- and Tnfr2-Deficient Animals

The above results prompted us to evaluate whether pharmacological inhibition of Duox1 using the NADPH oxidase inhibitor dibenziodolium chloride (DPI), which has been shown to inhibit Duox1 and H_2O_2 gradient formation in zebrafish [31,34], may

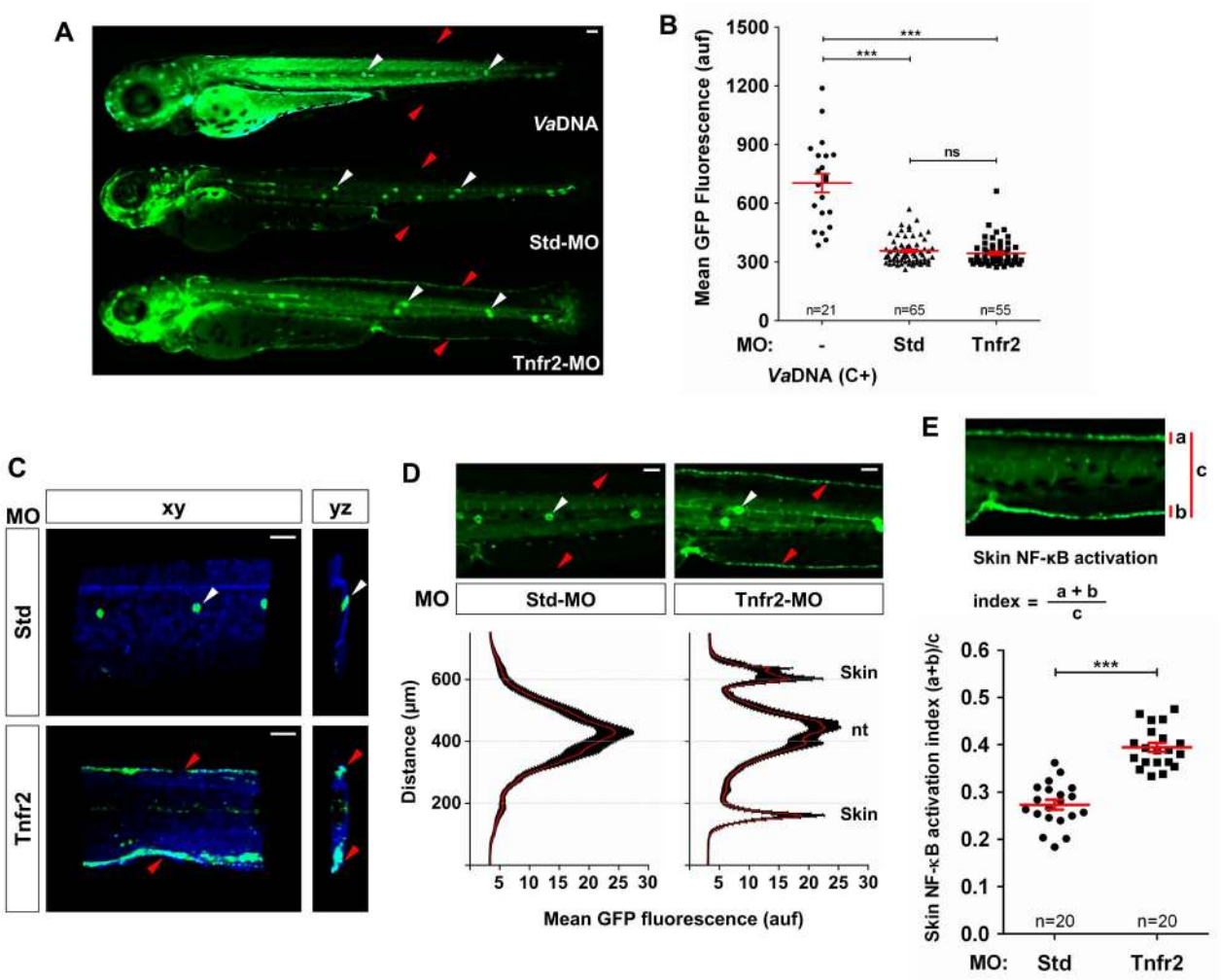

Figure 3. Tnfa and Tnfr2 deficiencies result in skin NF-κB activation. Zebrafish one-cell *NF-κB:eGFP* (A, B, D, E) or *NF-κB:eGFP*; *krt18:RFP* (C) embryos were injected with standard control (Std) or Tnfr2 MOs alone or in the presence of 2.3 ng/egg of *V. anguillarum* genomic DNA (VaDNA), as a positive control for NF-κB activation. (A) Representative pictures showing the induction of NF-κB activation in the skin (red arrowheads) of Tnfr2-deficient larvae at 72 hpf and the ubiquitous, strong induction in their VaDNA-injected siblings. Note the strong expression of NF-κB in neuromasts of control larvae (white arrowheads). (B) The mean GFP fluorescence was quantified in whole larvae, and no significant differences between Tnfr2-morphants and control larvae were observed. Each dot represents the mean GFP fluorescence per single larva. The mean ± S.E.M. of the whole GFP fluorescence for each group of larvae is also shown. (C) Representative frontal (*xy*) and lateral (*yz*) views of tridimensional reconstructions from confocal microscopy images of WIHC of *NF-κB:eGFP*; *krt18:RFP* larvae stained at 3 dpf with anti-RFP antibodies (keratinocytes, blue) showing the induction of NF-κB in the skin (eGFP, green) of Tnfr2-deficient larvae. (D, E) Quantification of NF-κB activation in the skin of Tnfr2-deficient larvae at 72 hpf. (D) Fluorescence intensity was measured in the area indicated of wild-type and Tnfr2-deficient larvae, as explained in the legend to Figure 1 (15 larvae per treatment from 3 different experiments). The skin and the neuromasts have been labeled to facilitate the larval orientation. Note the activation of NF-κB in the skin of Tnfr2-deficient larvae. (E) The skin NF-κB activation index was defined as the fluorescence in the skin (a+b) relative to the total fluorescence of the whole larvae (c). Each dot represents the skin NF-κB activation index per single larva. The mean ± S.E.M. of the skin NF-κB activation index for each group of larvae is also shown. Scale bars, 100 µm. ns, not significant; auf, arbitrary units of fluorescence. *$p<0.05$; **$p<0.01$; ***$p<0.001$.

doi:10.1371/journal.pbio.1001855.g003

restore skin homeostasis in Tnfa- and Tnfr2-deficient larvae. The results showed that DPI treatment completely inhibited the generation of H_2O_2 in the skin (Figure 5B,C), the infiltration of neutrophils (Figure 6A–C) into this tissue, and more importantly, skin NF-κB activation (Figure 6D–F) in both Tnfa- and Tnfr2-deficient animals. Collectively, these results demonstrate that the Tnfa/Tnfr2 axis is indispensable for skin homeostasis and its inhibition results in the release of Duox1-derived H_2O_2, local activation of NF-κB, induction of genes encoding Duox1 and pro-inflammatory mediators, and neutrophil infiltration.

DUOX1 Is Induced in Human Psoriasis and Lichen Planus Lesions

The crucial role of Duox1-generated H_2O_2 in the infiltration of neutrophils into the skin and the induction of NF-κB prompted us to investigate if this inflammatory signal may also play a role in human psoriasis and lichen planus. We analyzed by immunohistochemistry 10 healthy skins and 8 lichen planus and 15 psoriasis lesions using an antibody to human DUOX1 (Figure 7). The results showed that although DUOX1 was expressed at low levels in healthy epidermis, mainly in the granular layer, a drastic

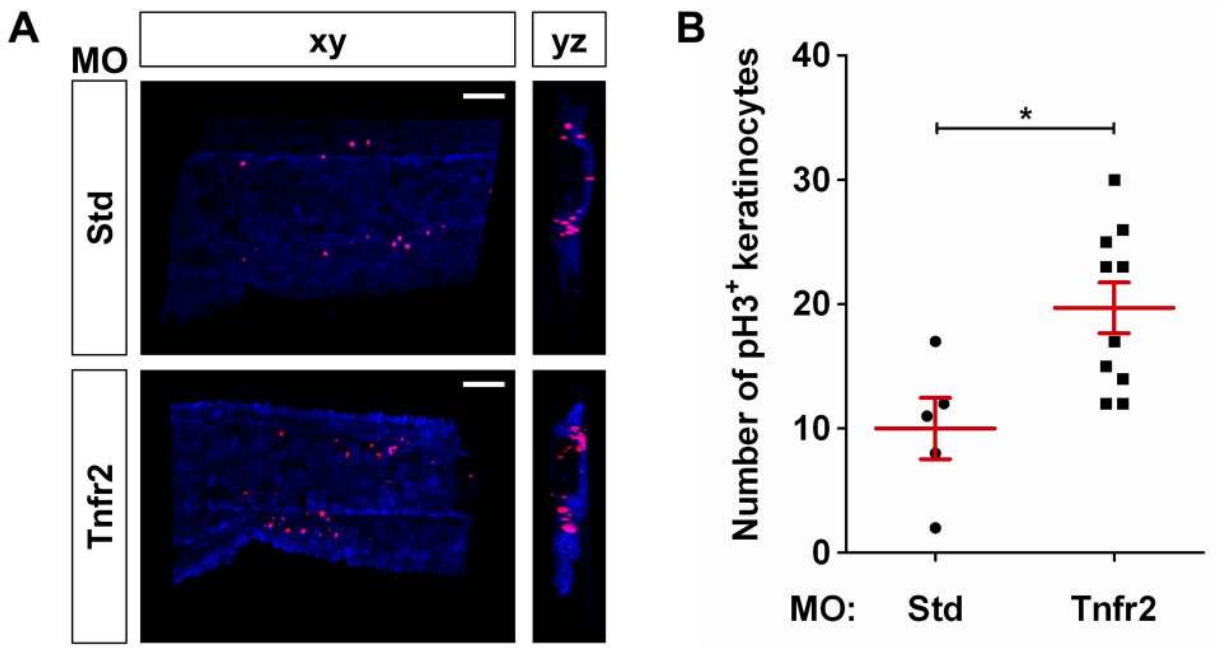

Figure 4. Tnfr2 deficiency results in increased proliferation of skin keratinocytes. Zebrafish one-cell *krt18:RFP* embryos were injected with standard control (Std) or Tnfr2 MOs. (A) Representative frontal (*xy*) and lateral (*yz*) tridimensional reconstructions from confocal microscopy images of WIHC of *krt18:RFP* larvae stained at 3 dpf with anti-RFP (keratinocytes, blue) and anti-phosphorylated H3 (pH 3, proliferation marker) antibodies. (B) Quantification of the number of pH3/RFP$^+$ (i.e., proliferating keratinocytes) cells in the CHT area. Each dot represents one single larva, and the mean ± S.E.M. for each group of larvae is also shown. Scale bars, 100 μm. *$p<0.05$.
doi:10.1371/journal.pbio.1001855.g004

induction of this enzyme was obvious in the keratinocytes of the spinous layer of the epidermis from both psoriasis and lichen planus lesions. In some patients, the induction was obvious in all keratinocytes of the spinous layer, whereas in others it was observed only in the upper layers of this stratum. It was noticeable the localization of DUOX1 in the plasma membrane of psoriasis and lichen planus keratinocytes and also in their cytoplasm, where it was accumulated in the upper side of these cells—that is, facing the cornified layer. Although this particular distribution deserves further investigation, these results strongly suggest a role for DUOX1 in psoriasis and lichen planus.

Discussion

Increased production of TNFα is associated with the development of autoimmune/chronic inflammatory diseases, including psoriasis, lichen planus, rheumatoid arthritis, and IBD. We have used the unique advantages of the zebrafish embryo for *in vivo* imaging and cell tracking to demonstrate that the genetic depletion of Tnfa or Tnfr2, but not Tnfr1, caused the infiltration of neutrophils into the skin and hyperproliferation of keratinocytes through the activation of an H_2O_2/NF-κB/Duox1 positive feedback inflammatory loop (Figure 8). Strikingly, neutrophils, but not macrophages, are rapidly attracted to the skin. However, the activation of NF-κB and the induction of the gene encoding Il1b in the skin occurred before the appearance of the first neutrophils in the developing embryo. More importantly, DUOX1 was also strongly induced in the skin lesions of psoriasis and lichen planus patients. Collectively, these results (i) indicate a critical role of TNFα/TNFR2 signaling in the protection of the skin against oxidative stress, (ii) might explain the appearance of psoriasis and lichen planus in patients treated with anti-TNFα therapies [5–10], and (iii) support the idea that specific inhibition of the TNFα/TNFR1 signaling axis while leaving TNFα/TNFR2 signaling unaffected would inhibit the pathological effects of TNFα and reduce the side effects associated with this therapy [19,36]. This apparent discrepancy with TNFα-deficient mice, which do not show skin inflammation, may be due to developmental and/or physiological compensations, which probably do not exist in humans [37–39].

One of the most intriguing observations from this study is that impaired Tnfr2 signaling led to the induction of *duox1* and the production of H_2O_2 by keratinocytes. H_2O_2 gradient was recently shown to contribute to the early influx of neutrophils in wound [31] and tumor [32], although it seems to be dispensable for neutrophil detection of localized infection [33]. To the best of our knowledge, this is the first study showing a role for Duox1-derived H_2O_2 in the induction of NF-κB in the skin *in vivo*, suggesting that H_2O_2 might play a critical role in the initiation and maintenance of chronic inflammatory diseases in both zebrafish and human. These observations suggest that antioxidants or inhibition of Duox1 might be therapeutic for the treatment of patients suffering from psoriasis, lichen planus, and other inflammatory diseases. Supporting this notion, several studies using psoriasis and IBD mouse models have shown that transgenic overexpression of endogenous antioxidant genes promotes protection, while antioxidant gene knockout promotes sensitization (reviewed by [40,41]). Even more importantly, the antioxidant levels and the oxidative stress biomarkers are usually correlated with the disease severity and the extent of inflammation in the psoriasis and IBD patients [40–42]. Therefore, all these results taken together suggest that antioxidants should be considered as part of a more specific and effective therapy for the treatment of inflammatory skin diseases, including psoriasis and lichen planus. The ability of Duox1

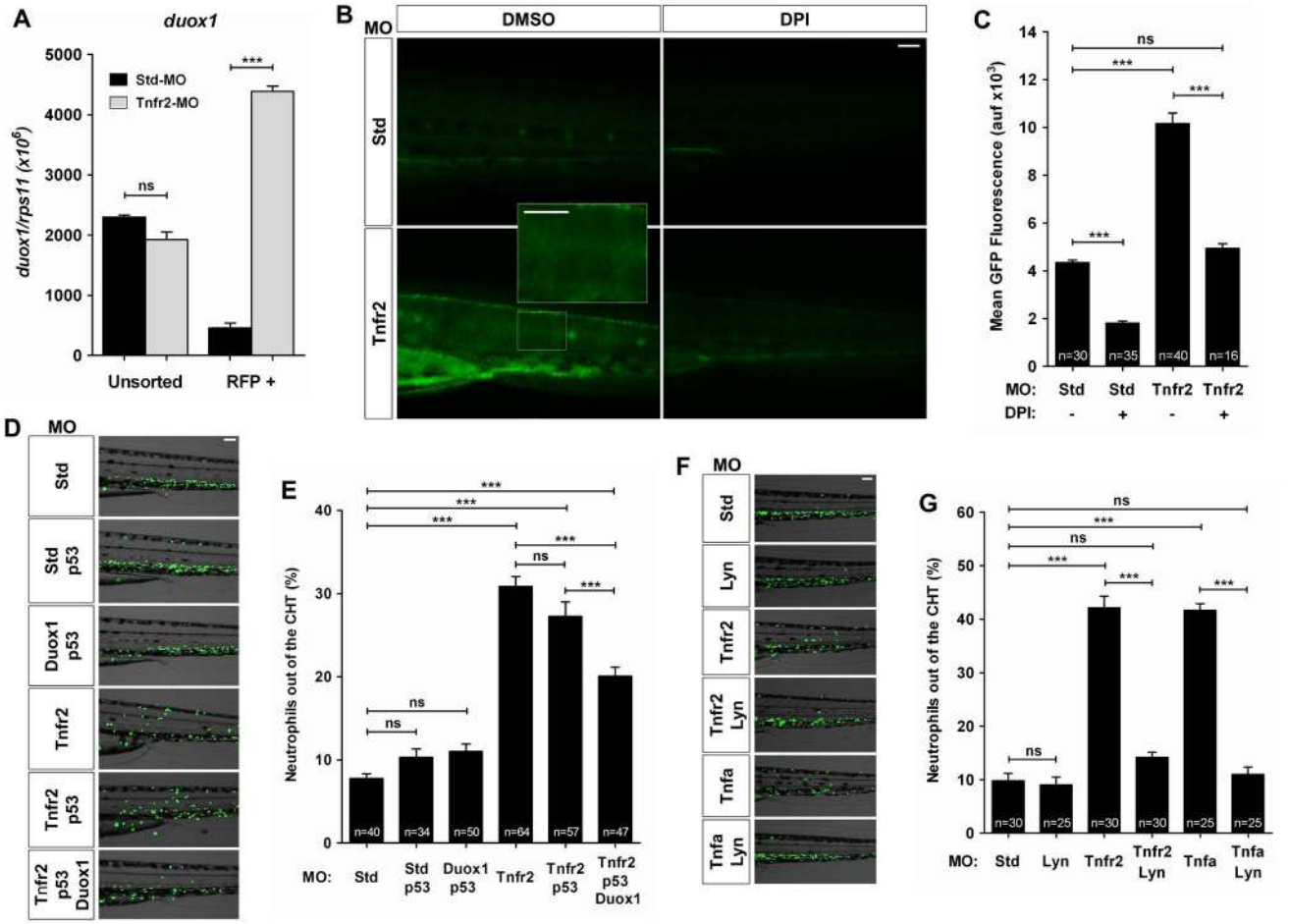

Figure 5. Tnfa and Tnfr2 deficiencies result in the Duox1-derived H_2O_2 production by keratinocytes. Zebrafish one-cell *krt18:RFP* (A), wild-type (B, C), or *mpx:eGFP* (D–G) embryos were injected with standard control (Std), Tnfr2, Tnfa, Duox1/p53, and/or Lyn MOs. (A) The expression of the *duox1* gene was measured by RT-qPCR in FACS-sorted keratinocytes from 72 hpf wild-type and Tnfr2-deficient larvae. (B, C) Wild-type and Tnfr2-deficient larvae were dechorionated at 24 hpf and treated by immersion in 100 μM DPI or vehicle alone (DMSO) for 24 h and then labeled with 50 μM acetyl-pentafluorobenzene sulphonyl fluorescein. Representative images of green channels of Std and Tnfr2 morphants are shown. Note that single keratinocytes are labeled with the H_2O_2 probe in Tnfr2-deficient larvae (inset). (D–G) Rescues with Duox1 (D, E) and Lyn (F, G) MOs at 72 hpf. The differences in the neutrophil distribution (D, F) and quantification of neutrophil mobilization from the CHT to the skin in the indicated number of larvae per group from three different experiments (E, G) are shown. The mean ± S.E.M. for each group is shown. Scale bars, 100 μm. ns, not significant. ***$p<0.001$.
doi:10.1371/journal.pbio.1001855.g005

inhibition by pharmacological approaches, but not of IL-1β, to restore skin homeostasis in Tnfa- and Tnfr2-deficient zebrafish embryos further supports this conclusion.

It is known that different reactive oxygen species (ROS) act as second messengers, influencing various cellular signal transduction pathways, including NF-κB. However, there are still many inconsistencies concerning the influence of oxidative stress on NF-κB activity [43], and unfortunately, most studies have been performed *in vitro* using H_2O_2 and cultured cells [44,45]. Such studies have shown that H_2O_2 can act as an activator of IκB kinases (IKKs) [46] or can inactivate these proteins [47], probably depending on the cell type. More recently, it has been found that the same prolyl hydroxylases that confer oxygen sensitivity to the hypoxia-inducible factor (HIF) pathway, namely PHD1 and PHD2, seem to act as repressors of the canonical NF-κB pathway through mechanisms that could include direct hydroxylation of IKKβ [48]. Our epistasis study in zebrafish demonstrates for the first time that the absence of Tnfa/Tnfr2 signaling led to the production of H_2O_2 by keratinocytes, which, in turn, resulted in NF-κB activation and the induction of genes encoding pro-inflammatory mediators. This self-perpetuating cycle may be of clinical importance in view of the presumably key role played by oxidative stress [40–42], HIF [49,50], and NF-κB in psoriasis and IBD. It is tempting to speculate that the Tnfa/Tnfr2 axis would be required to prevent skin oxidative stress through the regulation of ROS-detoxifying enzymes, as it has been reported for oligodendrocyte progenitor cells *in vitro* [51]. The model reported here might contribute to clarify the mechanisms involved in the regulation of oxidative stress by TNFα, the regulation of NF-κB activity by ROS, and the crosstalk between oxidative stress and inflammation *in vivo*.

The essential role played by NF-κB in the homeostasis of the skin is evidenced by the human X-linked genodermatosis IP, which affects the regulatory subunit of IKK (IKKγ, NEMO) [17]. Humans suffering from this genetic disease exhibit severe skin inflammation, paradoxically due to impaired NF-κB activation

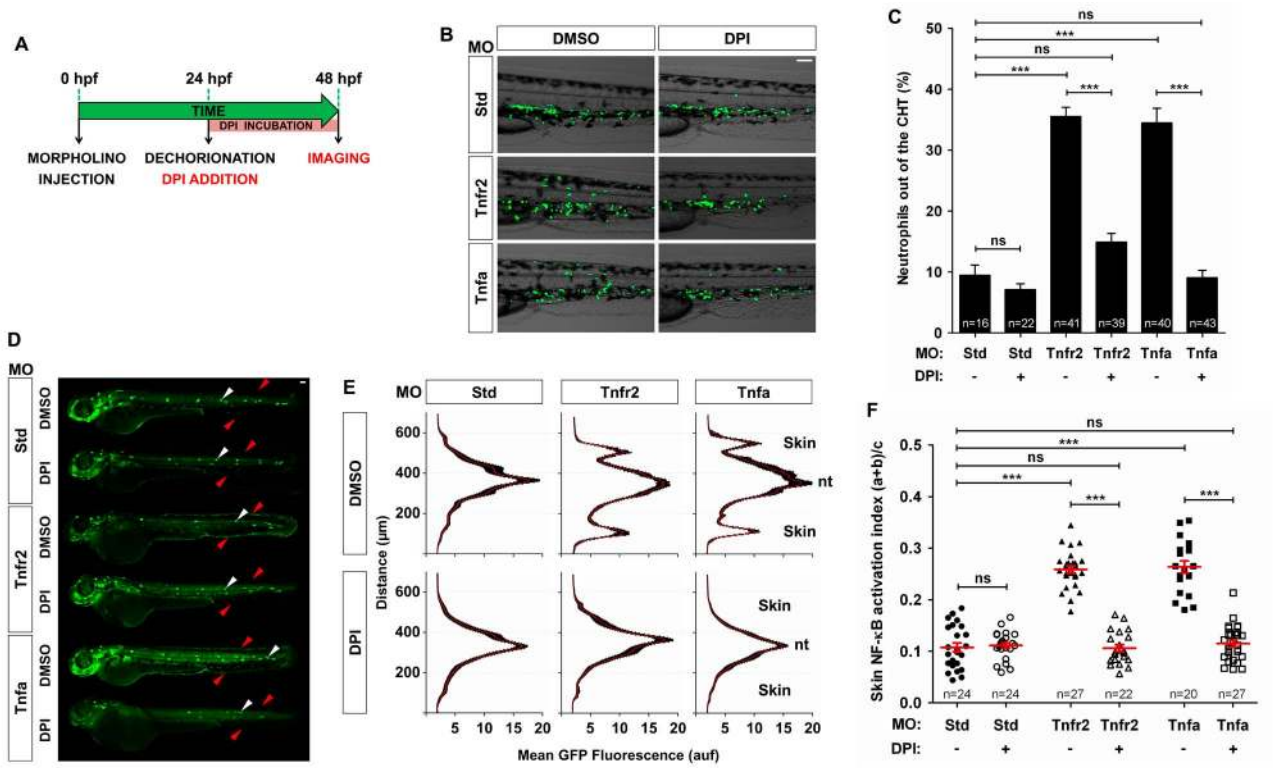

Figure 6. Pharmacological inhibition of Duox1 prevents skin inflammation in Tnfa- and Tnfr2-deficient zebrafish. Zebrafish one-cell *mpx:eGFP* (B, C) and *NF-κB:eGFP* (D–F) embryos were injected with standard control (Std), Tnfr2, or Tnfa MOs. (A) Scheme showing the experimental procedure: embryos were dechorionated at 24 hpf and treated by immersion in 100 µM DPI or vehicle alone (DMSO) for 24 h. (B, C) Representative images of bright field and green channels of the morphants at 48 hpf showing the differences in the neutrophils distribution (B) and quantification of neutrophil mobilization from the CHT to the skin in the indicated number of larvae per group from three different experiments (C). (D–F) Quantification of NF-κB activation in the skin of Tnfr2- and Tnfa-deficient larvae at 72 hpf. (E) Fluorescence intensity was measured for all the groups in the area indicated, as explained in the legend to Figure 1 (15 larvae per treatment from 3 different experiments). The skin and the notochord (nt) have been labeled to facilitate the larval orientation. Note the activation of NF-κB in the skin (red arrowheads) of Tnfr2-deficient larvae. Note the strong expression of NF-κB in neuromasts (white arrowheads). (F) Skin NF-κB activation index was defined as the fluorescence in the skin (a+b) relative to the total fluorescence of the whole larvae (c). Each dot represents the skin NF-κB activation index per single larva. The mean ± S.E.M. of the skin NF-κB activation index for each group of larvae is also shown. Scale bars, 100 µm. ns, not significant. ***$p<0.001$.
doi:10.1371/journal.pbio.1001855.g006

and reduced resistance to TNFα/TNFR1-mediated apoptosis [52,53]. Similarly, although NF-κB actively participates in the excessive inflammatory response observed in IBD patients [54,55], recent studies with mice defective in NF-κB activation have revealed that epithelial NF-κB activation is essential to preserve intestinal homeostasis [56,57]. Therefore, a critical NF-κB signaling balance is required for skin and gut homeostasis, as both excessive and defective epithelial NF-κB activation can result in inflammation. Similarly, although the TNFα/TNFR1 axis was earlier appreciated to be involved in the apoptosis of both keratinocytes and enterocytes in the absence of NF-κB signaling [52,53,56,57], our results show that TNFα signaling through TNFR2 is also critically required for skin homeostasis. Whether the TNFα/TNFR2 axis is also required for gut homeostasis will require further investigation using germ-free and gnotobiotic zebrafish larvae, as host–microbe interactions have a profound impact in gut physiology and are usually involved in IBD.

In conclusion, we have found that Tnfa signaling through Tnfr2 is indispensably required for the protection of the skin against oxidative stress-induced inflammation in the zebrafish. Thus, the absence of this signal triggers the local production of H_2O_2 by Duox1, which, in turn, activates NF-κB and results in the up-regulation of genes encoding pro-inflammatory mediators and neutrophil infiltration. These results, together with the induction of DUOX1 in the skin lesions of psoriasis and lichen planus patients, reveal a crucial role of H_2O_2 and DUOX1 in skin inflammation and suggest that pharmacologic and genetic therapies that target these two key factors could provide innovative approaches to the management of psoriasis, lichen planus, and other chronic inflammatory diseases.

Materials and Methods

Ethics Statement

The experiments performed comply with the Guidelines of the European Union Council (86/609/EU). Experiments and procedures were performed as approved by the Bioethical Committee of the University of Murcia (approval no. 537/2011) and the Ethical Clinical Research Committee of the University Hospital Virgen de la Arrixaca (approval no. 8/13).

Animals

Zebrafish (*Danio rerio* H.) were obtained from the Zebrafish International Resource Center and mated, staged, raised, and processed as described [58]. The lines *Tg(mpx:eGFP)*^{i114} [59], Tg(*lyz:dsRED*)^{nz50} [60], Tg(*mpeg1:eGFP*)^{gl22} [61], and *Tg(krt18:RFP)*

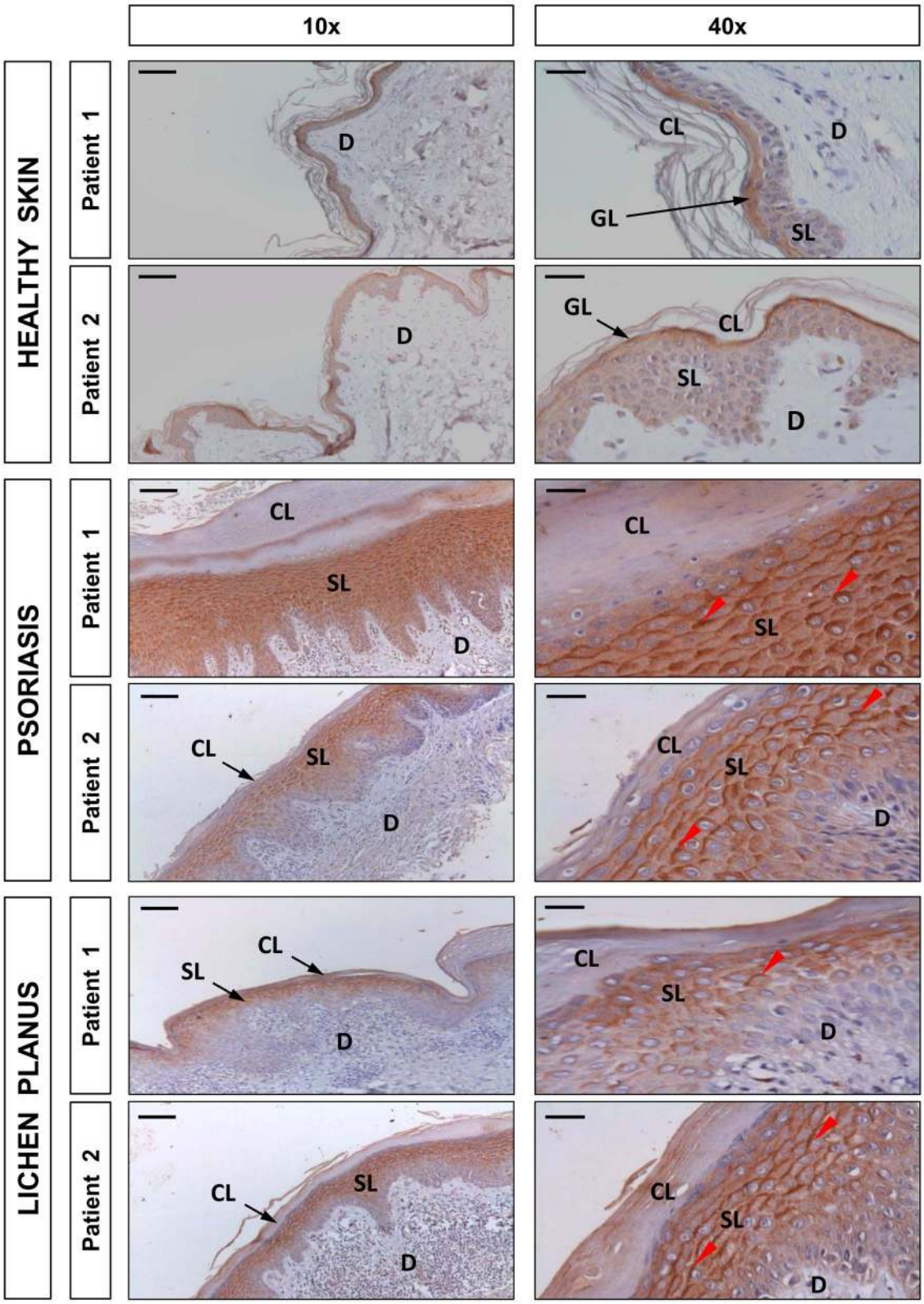

Figure 7. DUOX1 is induced in human psoriasis and lichen planus lesions. Representative images of sections from two healthy, two psoriatic, and two lichen planus skin biopsies that have been immunostained with an anti-DUOX1 goat polyclonal antibody and then slightly counterstained with hematoxilin. Note that DUOX1 is weakly expressed in healthy epidermis, mainly in the granular layer (GL), whereas it is strongly expressed (red arrowheads) in the spinous layer (SL) of both psoriasis and lichen planus lesions. CL, cornified layer; D, dermis. Scale bars, 100 μm (left panel) and 30 μm (right panel).
doi:10.1371/journal.pbio.1001855.g007

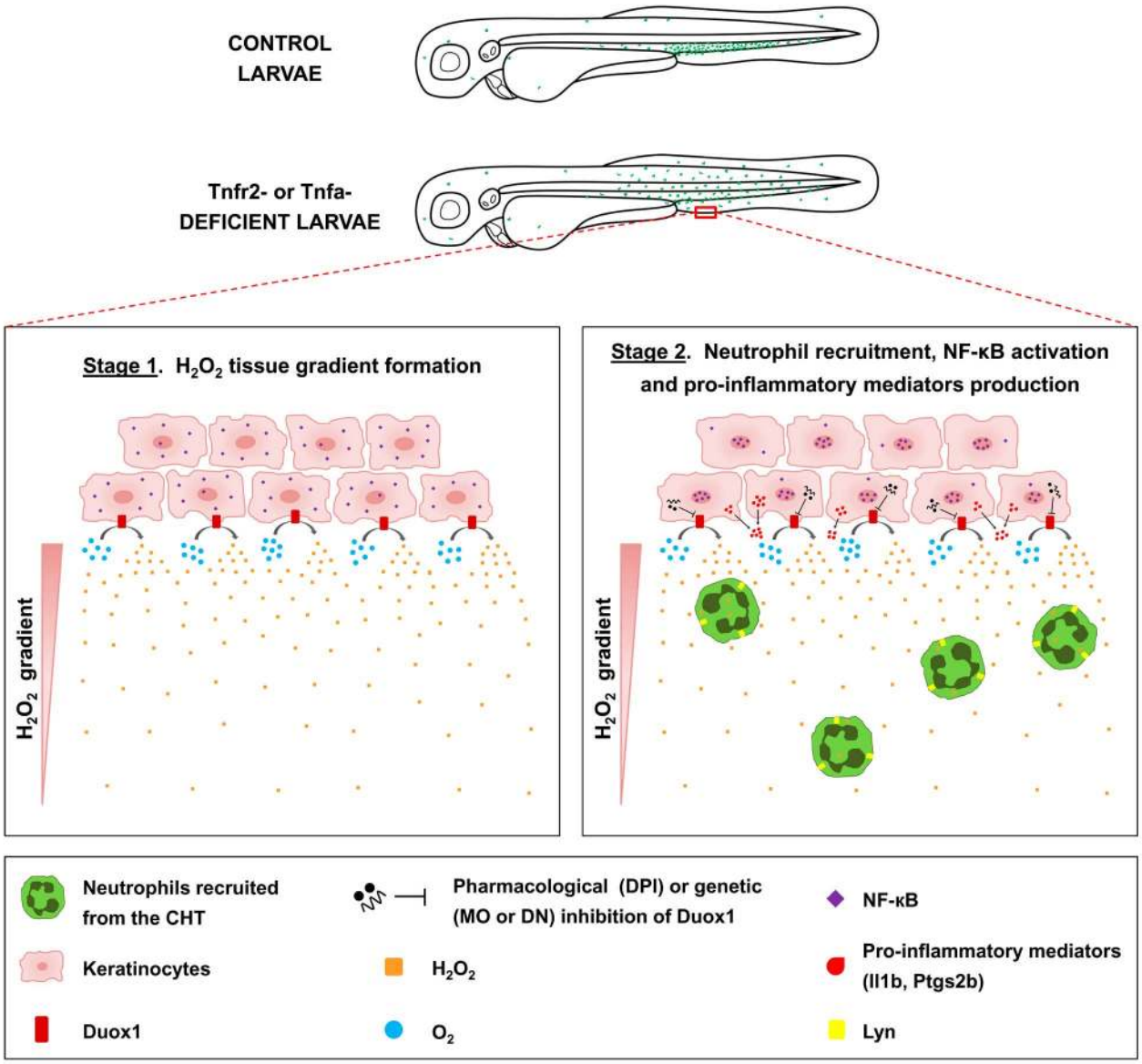

Figure 8. Proposed model illustrating the H_2O_2/NF-κB/Duox1 positive feedback inflammatory loop triggered in the skin of Tnfa- or Tnfr2-deficient zebrafish. Stage 1 (left panel): Tnfa or Tnfr2 deficiency triggers Duox1-dependent release of H_2O_2, which in turn promotes Lyn-mediated neutrophil infiltration. Stage 2 (right panel): H_2O_2 induces the activation of NF-κB, which is then translocated to the nucleus and induces the activation of genes encoding pro-inflammatory mediators (Il1b, Ptgs2, and probably Duox1). Pharmacological or genetic inhibition of Duox1 restores skin homeostasis.
doi:10.1371/journal.pbio.1001855.g008

[62] were previously described. The *Tg(NFκB-RE*:eGFP) (*NF-κB:eGFP* for simplicity) line was generated with the method and constructs previously described [28].

MO, RNA Injection, and Chemical Treatments

Specific MOs (Gene Tools) were resuspended in nuclease-free water to 1 mM (Table S1). *In vitro*–transcribed RNA was obtained following the manufacturer's instructions (mMESSAGE mMACHINE Kit, Ambion). MOs and RNA (200 pg/egg) were mixed in microinjection buffer (0.5× Tango buffer and 0.05% phenol red solution) and microinjected into the yolk sac of one- to eight-cell-stage embryos using a microinjector (Narishige) (0.5–1 nl per embryo). The same amounts of MOs and/or RNA were used in all experimental groups. The efficiency of the MOS was checked by RT-PCR as described previously [19,27,31,34].

In some experiments, 1 dpf embryos were manually dechorionated and/or treated for 24 h at 28°C by bath immersion with the NADPH oxidase inhibitor dibenziodolium chloride (DPI, Sigma-Aldrich) at a final concentration of 100 µM diluted in egg water supplemented with 1% DMSO.

Live Imaging of Zebrafish Larvae

At 72 hpf, larvae were anesthetized in tricaine and mounted in 1% (wt/vol) low-melting-point agarose (Sigma-Aldrich) dissolved in egg water [63]. Images were captured with an epifluorescence Lumar V12 stereomicroscope equipped with green and red fluorescent filters while animals were kept in their agar matrixes at 28.5°C. All images were acquired with the integrated camera on the stereomicroscope and were used for subsequently counting the number of neutrophils (*mpx:eGFP*) and examining their distribu-

tion. The activation of NF-κB was visualized and quantified using the line *NF-κB*::eGFP. Stacked images were captured using 1 µm (neutrophil infiltration into the skin) or 25 µm (neutrophil distribution, NF-κB activation, and H_2O_2 formation) increments and deconvolved using Huygens Essential Confocal software (v 4.1 0p6b) by Scientific Volume Imaging. Stacks were processed using the free source software ImageJ (http://rsbweb.nih.gov/ij) to obtain a maximum intensity projection of the *xy* axis of the stack. For the quantification of neutrophil distribution and NF-κB activation, the maximum projection for each larva was then converted to a fluorescence value matrix, where the value obtained for each pixel transversally was the mean ± S.E.M. for all the pixels for each row (15 larvae per treatment from 3 different experiments). In parallel, the activation of NF-κB in the skin was also quantified by the skin NF-κB activation index, which was defined as the fluorescence in the skin (a+b) relative to the total fluorescence of the larvae (c).

H_2O_2 imaging using a live cell fluorogenic substrate was performed essentially as previously described [32]. Briefly, 3-dpf tnfα and Tnfr2 morphants and their control siblings were loaded for 30 min with 50 µM acetyl-pentafluorobenzene sulphonyl fluorescein (Cayman Chemical) in 1% DMSO in egg water and imaged as above. As a positive control, complete transfection of the tail of anesthetized 72 hpf larvae was performed with a disposable sterile scalpel [63].

Flow Cytometry

At 3 dpf, approximately 300 to 500 *Tg(mpx:eGFP) and Tg(krt18:RFP)* larvae were anesthetized in tricaine, minced with a razor blade, incubated at 28°C for 30 min with 0.077 mg/ml Liberase (Roche), and the resulting cell suspension passed through a 40 µm cell strainer. Sytox (Life Technologies) was used as a vital dye to exclude dead cells. Flow cytometric acquisitions were performed on a FACSCALIBUR (BD), and cell sorting was performed on a Coulter (Epics Altra). Analyses were performed using FlowJo software (Treestar).

Analysis of Gene Expression

Total RNA was extracted from whole embryos/larvae or sorted cell suspensions with TRIzol reagent (Invitrogen) following the manufacturer's instructions and treated with DNase I, amplification grade (1 U/µg RNA; Invitrogen). SuperScript III RNase H^- Reverse Transcriptase (Invitrogen) was used to synthesize first-strand cDNA with oligo(dT)18 primer from 1 µg of total RNA at 50°C for 50 min. Real-time PCR was performed with an ABI PRISM 7500 instrument (Applied Biosystems) using SYBR Green PCR Core Reagents (Applied Biosystems). Reaction mixtures were incubated for 10 min at 95°C, followed by 40 cycles of 15 s at 95°C, 1 min at 60°C, and finally 15 s at 95°C, 1 min 60°C, and 15 s at 95°C. For each mRNA, gene expression was normalized to the ribosomal protein S11 (*rps11*) content in each sample using the Pfaffl method [64]. The primers used are shown in Table S2. In all cases, each PCR was performed with triplicate samples and repeated at least with two independent samples.

Histology and WIHC

Larvae were fixed overnight in 4% paraformaldehyde solution (PFA), embedded in Paraplast Plus (Sherwood Medical), and sectioned at a thickness of 5 µm. After being dewaxed and rehydrated, they were stained with haematoxylin and eosin (H&E).

Tg(*mpx:eGFP*) or Tg(NF-κB:eGFP); *Tg(krt18:RFP)* 3 dpf larvae were fixed overnight at 4°C in 4% PFA at room temperature, dehydrated in methanol/PBS solutions (25, 50, 75, and 100%, 5 min each), and stored in 100% methanol at −20°C. For staining, larvae were rehydrated in 75, 50, and 25% methanol/PBT (PBS and 0.1% Tween-20) solutions for 5 min each, washed three times for 5 min in PBT, incubated for 5 min RT with 150 mM Tris-HCl pH 9, followed by heating at 70°C for 15 min [65]. After the heating treatment, larvae were directly washed twice in PBT for 10 min and twice in dH_2O for 5 min. Subsequently, to enhance tissue permeabilization, larvae were incubated with cold acetone for 20 min at −20°C, washed twice in dH_2O and twice in PBT (5 min each), followed by blocking with blocking solution (PDT = PBT+1% DMSO) supplemented with 5% FBS and 2 mg/ml BSA) for 2 h at 22°C. After blocking, embryos were incubated overnight at 4°C with primary antibodies diluted (1:200) in blocking buffer, washed three times in PDT (15 min each), and blocked again for 2 h at 22°C. Secondary antibody staining was done for 2 h RT at 1:500 dilution in blocking buffer, and larvae were then washed five times in PBT (5 min each) and stored in Vectashield (Vector Labs) until image acquisition. The following primary antibodies were used: rabbit anti-phosphorylated-Histone H3 (Ser 10)-R (#SC8656-R, Santa Cruz Biotechnology) and rabbit anti-human p63 (#SC8343, Santa Cruz Biotechnology). Mouse anti-RFP (#MA5-15257, Thermo Scientific) and Alexa Fluor 594 (#A11032) and Alexa Fluor 532 (#A11002) Goat Anti-Mouse IgG (H+L) (Life Technologies) were used as secondary antibodies.

Confocal immunofluorescence images were acquired with a confocal microscope (LEICA TCS-SP2, Leica) using an NA 0.70/20× dry objective. Z-series were acquired using a 210–300 µm pinhole. The 2D and 3D maximum intensity projections and corresponding animation videos were made using ImageJ (http://rsb.info.nih.gov/ij/).

Human Skin Samples

Skin biopsies from healthy donors ($n = 10$) and lichen planus ($n = 8$) and psoriasis patients ($n = 15$) were fixed in 4% PFA, embedded in Paraplast Plus, and sectioned at a thickness of 5 µm. After being dewaxed and rehydrated, the sections were incubated in 50 mM glycine-HCl buffer (pH 3.5) containing 0.01% ethylenediaminetetraacetic acid (EDTA) at 95°C for 5 min and then at room temperature for 20 min to retrieve the antigen. Afterwards, they were immunostained with a 1/50 dilution of a goat polyclonal antibody to human DUOX1 (sc-48858, Santa Cruz Biotechnology) followed by ImmunoCruz goat ABC Staining System (sc-2023, Santa Cruz Biotechnology) following the manufacturer's recommendations. The specificity of the staining was confirmed by pre-incubating a 10-fold excess (in molarity) of a commercial blocking peptide (sc-48858 P, Santa Cruz Biotechnology) with the DUOX1 antibody overnight at 4°C. No staining was observed in these conditions. Sections were finally examined under a Leica microscope equipped with a digital camera Leica DFC 280, and the photographs were processed with Leica QWin Pro software.

Statistical Analysis

Data were analyzed by analysis of variance (ANOVA) and a Tukey multiple range test to determine differences between groups. The differences between two samples were analyzed by the Student *t* test. The contingency graphs were analyzed by the Chi-square (and Fisher's exact) test.

Supporting Information

Figure S1 Tnfa and Tnfr2 deficiencies result in neutrophil mobilization. Zebrafish one-cell *mpx:eGFP* embryos were injected with standard control (Std), Tnfr1, Tnfr2, Tnfa, or Tnfr1+Tnfr2 MOs alone or combination with antisense (As), Tnfa, Tnfr2, or

DN-Tnfr2 mRNAs. The phenotype of 3 dpf larvae was classified as neutrophil grouped in the CHT or scattered, as described in Figure 1. ***$p<0.001$.
(TIF)

Figure S2 Macrophage distribution is not altered in Tnfa- or Tnfr2-deficient larvae. Zebrafish one-cell *mpeg1:eGFP* embryos were injected with standard control (Std), Tnfr2, and Tnfa MOs. Representative images showing macrophage distribution in 72 hpf larvae. Scale bars, 100 μm.
(TIF)

Figure S3 Efficiency of sorting of neutrophils and keratinocytes. Zebrafish one-cell *mpx*:eGFP (A) or *krt18*:RFP (B) embryos were injected with standard control (Std) or Tnfr2 MOs. Neutrophils (A) and keratinocytes (B) were FACS-sorted from 72 hpf larvae, and the expression of *gfp* and *mpx* (A) and *krt18* and *p63* (B) genes was measured by RT-qPCR in unsorted and sorted cells. The data are shown as the mean ± S.E.M. ns, not significant. *$p<0.05$; ***$p<0.001$.
(TIF)

Figure S4 Neutrophils and keratinocytes expressed both Tnf receptors. Neutrophils (A) and keratinocytes (B) were FACS-sorted from 72 hpf *mpx:eGFP* and *krt18:RFP* larvae, respectively, and the expression of *tnfr1* and *tnfr2* genes was measured by RT-qPCR in unsorted and sorted cells. The data are shown as the mean ± S.E.M. ns, not significant. **$p<0.01$; ***$p<0.001$.
(TIF)

Figure S5 IL-1β is induced in Tnfr2-deficient embryos before the emergence of neutrophils. Zebrafish one-cell wild-type embryos were injected with standard control (Std) or Tnfr2 MOs. The expression of *il1b* gene was measured by RT-qPCR in whole embryos at 24 and 48 hpf. The data are shown as the mean ± S.E.M. *$p<0.05$.
(TIF)

Figure S6 The skin of Tnfr2-deficient larvae does not show histopathological alterations. Zebrafish one-cell embryos were injected with standard control (Std) or Tnfr2 MOs. At 3 (A) and 5 (B) dpf, the larvae were fixed, embedded in Paraplast Plus, sectioned at 5 μm, and stained with H&E. M, muscle. Arrowheads, skin. Scale bars, 50 μm.
(TIF)

Figure S7 Pharmacological inhibition of Duox1 inhibits H_2O_2 production after wounding. Zebrafish one-cell wild-type embryos were treated at 72 hpf by immersion in 100 μM DPI or vehicle alone (DMSO) in the presence of 50 μM acetyl-pentafluorobenzene sulphonyl fluorescein, and tailfins were then transected. Representative images of the formation of the H_2O_2 gradient at 1 h postwounding. Note that DPI treatment completely inhibits H_2O_2 formation at the wound. Scale bars, 100 μm.
(TIF)

Figure S8 H_2O_2 production by Tnfr2-deficient keratinocytes preceded the activation of NF-κB. Zebrafish one-cell wild-type (A, B) or *lyz:dsRED*; *NF-κB:eGFP* (C, D) embryos were injected with standard control (Std) or Tnfr2 MOs. (A, B) Larvae were dechorionated at 24 hpf and then labeled with 50 μM acetyl-pentafluorobenzene sulphonyl fluorescein at 24, 48, and 72 hpf. Representative images of green channels of Std and Tnfr2 morphants (A) and quantification of green fluorescence in the indicated number of larvae (B) are shown. Note that increased H_2O_2 production by skin keratinocytes is already observed at 24 hpf. (C) Representative pictures showing NF-κB activation levels in control and Tnfr2-deficient larvae at 24, 48, and 72 hpf. Note that NF-κB is induced in the skin (red arrowheads) of Tnfr2-deficient larvae at 48 h and that neutrophil dispersion is observed at 72 hpf and, to some extent, at 48 hpf. The neuromasts are indicated with white arrowheads. (D) Quantification of the percentage of larvae showing activation of the NF-κB in the skin. The results are shown as the mean ± S.E.M. The number of larvae analyzed is also indicated. Scale bars, 100 μm. ns, not significant; auf, arbitrary units of fluorescence. *$p<0.05$; **$p<0.01$; ***$p<0.001$.
(TIF)

Figure S9 Genetic inactivation of Duox1 using a DN form partially prevents neutrophil infiltration into the skin of Tnfa- and Tnfr2-deficient zebrafish. Zebrafish one-cell *mpx:eGFP* embryos were injected with standard control (Std), Tnfr2, or Tnfa MOs alone or combination with antisense (As) or DN-Duox1 mRNAs. Representative images of bright field and green channels of morphants at 72 hpf showing the differences in the neutrophils distribution (A) and quantification of neutrophil mobilization from the CHT to the skin in the indicated number of larvae per group from three different experiments (B). The mean ± S.E.M. for each group is shown. Scale bars, 100 μm. ns, not significant. ***$p<0.001$.
(TIF)

Table S1 MOs used in this study. The gene symbols followed the Zebrafish Nomenclature Guidelines (http://zfin.org/zf_info/nomen.html). ENA, European Nucleotide Archive (http://www.ebi.ac.uk/ena/).
(DOCX)

Table S2 Primers used in this study. The gene symbols followed the Zebrafish Nomenclature Guidelines (http://zfin.org/zf_info/nomen.html). ENA, European Nucleotide Archive (http://www.ebi.ac.uk/ena/).
(DOCX)

Video S1 Neutrophils infiltrate the skin in Tnfr2-deficient larvae. Animations of tridimensional projections obtained by laser confocal microscopy of STD morphants showing neutrophils in green (GFP) and basal keratinocytes in red (p63). See legend to Figure 1 for details.
(AVI)

Video S2 Neutrophils infiltrate the skin in Tnfr2-deficient larvae. Animations of tridimensional projections obtained by laser confocal microscopy of Tnfr2 morphants showing neutrophils in green (GFP) and basal keratinocytes in red (p63). See legend to Figure 1 for details.
(AVI)

Video S3 NF-κB is induced in the skin of Tnfr2-deficient larvae. Animations of tridimensional projections obtained by laser confocal microscopy of STD morphants showing NF-κB activity in green (GFP) and basal keratinocytes in blue (RFP). See legend to Figure 3 for details.
(AVI)

Video S4 NF-κB is induced in the skin of Tnfr2-deficient larvae. Animations of tridimensional projections obtained by laser confocal microscopy of Tnfr2 morphants showing NF-κB activity in green (GFP) and basal keratinocytes in blue (RFP). See legend to Figure 3 for details.
(AVI)

Acknowledgments

We thank I. Fuentes and P. Martínez for excellent technical assistance; Professors P Crosier and G Lieschke for the *lyz:dsRED* and *mpeg1:eGFP*

lines, respectively; and J. Muñoz and A. Bernabeu for the sorting of neutrophils and keratinocytes.

Author Contributions

The author(s) have made the following declarations about their contributions: Conceived and designed the experiments: SC SdO DG-M RE-P VM. Performed the experiments: SC SdO AL-M DG-M RE-P SDT MLC VM. Analyzed the data: SC SdO AL-M DG-M RE-P SDT MLC SAR RC-V IV-A JM MPS VM. Contributed reagents/materials/analysis tools: RC-V IV-A H-JT. Wrote the paper: VM.

References

1. Shalaby M R , Sundan A , Loetscher H , Brockhaus M , Lesslauer W , et al. (1990) Binding and regulation of cellular functions by monoclonal antibodies against human tumor necrosis factor receptors. J Exp Med 172: 1517–1520.
2. Aggarwal B B (2003) Signalling pathways of the TNF superfamily: a double-edged sword. Nat Rev Immunol 3: 745–756.
3. Faustman D , Davis M (2010) TNF receptor 2 pathway: drug target for autoimmune diseases. Nat Rev Drug Discov 9: 482–493.
4. Palladino M A , Bahjat F R , Theodorakis E A , Moldawer L L (2003) Anti-TNF-alpha therapies: the next generation. Nat Rev Drug Discov 2: 736–746.
5. Denadai R , Teixeira F V , Steinwurz F , Romiti R , Saad-Hossne R (2012) Induction or exacerbation of psoriatic lesions during anti-TNF-alpha therapy for inflammatory bowel disease: a systematic literature review based on 222 cases. J Crohns Colitis 7: 517–524.
6. Sherlock M E , Walters T , Tabbers M M , Frost K , Zachos M , et al. (2012) Infliximab-induced psoriasis and psoriasiform skin lesions in pediatric Crohn's disease and a potential association with IL-23 receptor polymorphisms. J Pediatr Gastroenterol Nutr 56: 512–518.
7. Asarch A , Gottlieb A B , Lee J , Masterpol K S , Scheinman P L , et al. (2009) Lichen planus-like eruptions: an emerging side effect of tumor necrosis factor-alpha antagonists. J Am Acad Dermatol 61: 104–111.
8. Battistella M , Rivet J , Bachelez H , Liote F (2008) Lichen planus associated with etanercept. Br J Dermatol 158: 188–190.
9. Fernandez-Torres R , Paradela S , Valbuena L , Fonseca E (2010) Infliximab-induced lichen planopilaris. Ann Pharmacother 44: 1501–1503.
10. Wendling D , Biver-Dalle C , Vidon C , Prati C , Aubin F (2013) Lichen planus under anti TNF therapy for ankylosing spondylitis. Joint Bone Spine 80: 227–228.
11. Kondo S , Sauder D N (1997) Tumor necrosis factor (TNF) receptor type 1 (p55) is a main mediator for TNF-alpha-induced skin inflammation. Eur J Immunol 27: 1713–1718.
12. Pasparakis M , Courtois G , Hafner M , Schmidt-Supprian M , Nenci A , et al. (2002) TNF-mediated inflammatory skin disease in mice with epidermis-specific deletion of IKK2. Nature 417: 861–866.
13. Gugasyan R , Voss A , Varigos G , Thomas T , Grumont R J , et al. (2004) The transcription factors c-rel and RelA control epidermal development and homeostasis in embryonic and adult skin via distinct mechanisms. Mol Cell Biol 24: 5733–5745.
14. Omori E , Matsumoto K , Sanjo H , Sato S , Akira S , et al. (2006) TAK1 is a master regulator of epidermal homeostasis involving skin inflammation and apoptosis. J Biol Chem 281: 19610–19617.
15. Sayama K , Hanakawa Y , Nagai H , Shirakata Y , Dai X , et al. (2006) Transforming growth factor-beta-activated kinase 1 is essential for differentiation and the prevention of apoptosis in epidermis. J Biol Chem 281: 22013–22020.
16. van Hogerlinden M , Rozell B L , Toftgard R , Sundberg J P (2004) Characterization of the progressive skin disease and inflammatory cell infiltrate in mice with inhibited NF-kappaB signaling. J Invest Dermatol 123: 101–108.
17. Smahi A , Courtois G , Vabres P , Yamaoka S , Heuertz S , et al. (2000) Genomic rearrangement in NEMO impairs NF-kappaB activation and is a cause of incontinentia pigmenti. The International Incontinentia Pigmenti (IP) Consortium. Nature 405: 466–472.
18. Roca F J , Mulero I , Lopez-Munoz A , Sepulcre M P , Renshaw S A , et al. (2008) Evolution of the inflammatory response in vertebrates: fish TNF-alpha is a powerful activator of endothelial cells but hardly activates phagocytes. J Immunol 181: 5071–5081.
19. Espin R , Roca F J , Candel S , Sepulcre M P , Gonzalez-Rosa J M , et al. (2013) TNF receptors regulate vascular homeostasis in zebrafish through a caspase-8, caspase-2 and P53 apoptotic program that bypasses caspase-3. Dis Model Mech 6: 383–396.
20. Murayama E , Kissa K , Zapata A , Mordelet E , Briolat V , et al. (2006) Tracing hematopoietic precursor migration to successive hematopoietic organs during zebrafish development. Immunity 25: 963–975.
21. Bennett C M , Kanki J P , Rhodes J , Liu T X , Paw B H , et al. (2001) Myelopoiesis in the zebrafish, Danio rerio. Blood 98: 643–651.
22. Le Guyader D , Redd M J , Colucci-Guyon E , Murayama E , Kissa K , et al. (2008) Origins and unconventional behavior of neutrophils in developing zebrafish. Blood 111: 132–141.
23. Dodd M E , Hatzold J , Mathias J R , Walters K B , Bennin D A , et al. (2009) The ENTH domain protein Clint1 is required for epidermal homeostasis in zebrafish. Development 136: 2591–2600.
24. Mathias J R , Dodd M E , Walters K B , Rhodes J , Kanki J P , et al. (2007) Live imaging of chronic inflammation caused by mutation of zebrafish Hai1. J Cell Sci 120: 3372–3383.
25. Carney T J , von der Hardt S , Sonntag C , Amsterdam A , Topczewski J , et al. (2007) Inactivation of serine protease Matriptase1a by its inhibitor Hai1 is required for epithelial integrity of the zebrafish epidermis. Development 134: 3461–3471.
26. Lieschke G J , Oates A C , Crowhurst M O , Ward A C , Layton J E (2001) Morphologic and functional characterization of granulocytes and macrophages in embryonic and adult zebrafish. Blood 98: 3087–3096.
27. Lopez-Munoz A , Sepulcre M P , Roca F J , Figueras A , Meseguer J , et al. (2011) Evolutionary conserved pro-inflammatory and antigen presentation functions of zebrafish IFNgamma revealed by transcriptomic and functional analysis. Mol Immunol 48: 1073–1083.
28. Kanther M , Sun X , Muhlbauer M , Mackey L C , Flynn E J , 3rd, et al. (2011) Microbial colonization induces dynamic temporal and spatial patterns of NF-kappaB activation in the zebrafish digestive tract. Gastroenterology 141: 197–207.
29. Alcaraz-Perez F , Mulero V , Cayuela M L (2008) Application of the dual-luciferase reporter assay to the analysis of promoter activity in Zebrafish embryos. BMC Biotechnol 8: 81.
30. Sepulcre M P , Alcaraz-Perez F , Lopez-Munoz A , Roca F J , Meseguer J , et al. (2009) Evolution of lipopolysaccharide (LPS) recognition and signaling: fish TLR4 does not recognize LPS and negatively regulates NF-kappaB activation. J Immunol 182: 1836–1845.
31. Niethammer P , Grabher C , Look A T , Mitchison T J (2009) A tissue-scale gradient of hydrogen peroxide mediates rapid wound detection in zebrafish. Nature 459: 996–999.
32. Feng Y , Santoriello C , Mione M , Hurlstone A , Martin P (2010) Live imaging of innate immune cell sensing of transformed cells in zebrafish larvae: parallels between tumor initiation and wound inflammation. PLoS Biol 8: e1000562.
33. Deng Q , Harvie E A , Huttenlocher A (2012) Distinct signalling mechanisms mediate neutrophil attraction to bacterial infection and tissue injury. Cell Microbiol 14: 517–528.
34. Yoo S K , Starnes T W , Deng Q , Huttenlocher A (2011) Lyn is a redox sensor that mediates leukocyte wound attraction in vivo. Nature 480: 109–112.
35. de Oliveira S , López-Muñoz A , Candel S , Pelegrín P , Calado A , et al. (2014) ATP modulates acute inflammation in vivo through Duox1-derived H_2O_2 production and NF-kB activation. J Immunol accepted.
36. Van Hauwermeiren F , Vandenbroucke R E , Libert C (2011) Treatment of TNF mediated diseases by selective inhibition of soluble TNF or TNFR1. Cytokine Growth Factor Rev 22: 311–319.
37. Inui A (2000) Transgenic study of energy homeostasis equation: implications and confounding influences. FASEB J 14: 2158–2170.
38. Maddison K , Clarke A R (2005) New approaches for modelling cancer mechanisms in the mouse. J Pathol 205: 181–193.
39. Rudmann D G , Durham S K (1999) Utilization of genetically altered animals in the pharmaceutical industry. Toxicol Pathol 27: 111–114.
40. Zhou Q , Mrowietz U , Rostami-Yazdi M (2009) Oxidative stress in the pathogenesis of psoriasis. Free Radic Biol Med 47: 891–905.
41. Zhu H , Li Y R (2012) Oxidative stress and redox signaling mechanisms of inflammatory bowel disease: updated experimental and clinical evidence. Exp Biol Med (Maywood) 237: 474–480.
42. Kim Y , Kim B H , Lee H , Jeon B , Lee Y S , et al. (2011) Regulation of skin inflammation and angiogenesis by EC-SOD via HIF-1alpha and NF-kappaB pathways. Free Radic Biol Med 51: 1985–1995.
43. Siomek A (2012) NF-kappaB signaling pathway and free radical impact. Acta Biochim Pol 59: 323–331.
44. Byun M S , Jeon K I , Choi J W , Shim J Y , Jue D M (2002) Dual effect of oxidative stress on NF-kappakB activation in HeLa cells. Exp Mol Med 34: 332–339.
45. Schreck R , Rieber P , Baeuerle P A (1991) Reactive oxygen intermediates as apparently widely used messengers in the activation of the NF-kappa B transcription factor and HIV-1. EMBO J 10: 2247–2258.
46. Kamata H , Manabe T , Oka S , Kamata K , Hirata H (2002) Hydrogen peroxide activates IkappaB kinases through phosphorylation of serine residues in the activation loops. FEBS Lett 519: 231–237.
47. Korn S H , Wouters E F , Vos N , Janssen-Heininger Y M (2001) Cytokine-induced activation of nuclear factor-kappa B is inhibited by hydrogen peroxide through oxidative inactivation of IkappaB kinase. J Biol Chem 276: 35693–35700.
48. Cummins E P , Berra E , Comerford K M , Ginouves A , Fitzgerald K T , et al. (2006) Prolyl hydroxylase-1 negatively regulates IkappaB kinase-beta, giving insight into hypoxia-induced NFkappaB activity. Proc Natl Acad Sci U S A 103: 18154–18159.

49. Rosenberger C , Solovan C , Rosenberger A D , Jinping L , Treudler R , et al. (2007) Upregulation of hypoxia-inducible factors in normal and psoriatic skin. J Invest Dermatol 127: 2445–2452.
50. Colgan S P , Taylor C T (2010) Hypoxia: an alarm signal during intestinal inflammation. Nat Rev Gastroenterol Hepatol 7: 281–287.
51. Maier O , Fischer R , Agresti C , Pfizenmaier K (2013) TNF receptor 2 protects oligodendrocyte progenitor cells against oxidative stress. Biochem Biophys Res Commun 440: 336–341.
52. Makris C , Godfrey V L , Krahn-Senftleben G , Takahashi T , Roberts J L , et al. (2000) Female mice heterozygous for IKK gamma/NEMO deficiencies develop a dermatopathy similar to the human X-linked disorder incontinentia pigmenti. Mol Cell 5: 969–979.
53. Nenci A , Huth M , Funteh A , Schmidt-Supprian M , Bloch W , et al. (2006) Skin lesion development in a mouse model of incontinentia pigmenti is triggered by NEMO deficiency in epidermal keratinocytes and requires TNF signaling. Hum Mol Genet 15: 531–542.
54. Ellis R D , Goodlad J R , Limb G A , Powell J J , Thompson R P , et al. (1998) Activation of nuclear factor kappa B in Crohn's disease. Inflamm Res 47: 440–445.
55. Schreiber S , Nikolaus S , Hampe J (1998) Activation of nuclear factor kappa B inflammatory bowel disease. Gut 42: 477–484.
56. Nenci A , Becker C , Wullaert A , Gareus R , van Loo G , et al. (2007) Epithelial NEMO links innate immunity to chronic intestinal inflammation. Nature 446: 557–561.
57. Kajino-Sakamoto R , Inagaki M , Lippert E , Akira S , Robine S , et al. (2008) Enterocyte-derived TAK1 signaling prevents epithelium apoptosis and the development of ileitis and colitis. J Immunol 181: 1143–1152.
58. Westerfield M (2000) The Zebrafish book. A guide for the laboratory use of zebrafish danio* (Brachydanio) rerio. Eugene, OR: University of Oregon Press.
59. Renshaw S A , Loynes C A , Trushell D M , Elworthy S , Ingham P W , et al. (2006) A transgenic zebrafish model of neutrophilic inflammation. Blood 108: 3976–3978.
60. Hall C , Flores M V , Storm T , Crosier K , Crosier P (2007) The zebrafish lysozyme C promoter drives myeloid-specific expression in transgenic fish. BMC Dev Biol 7: 42.
61. Ellett F , Pase L , Hayman J W , Andrianopoulos A , Lieschke G J (2011) mpeg1 promoter transgenes direct macrophage-lineage expression in zebrafish. Blood 117: e49–56.
62. Wang Y H , Chen Y H , Lin Y J , Tsai H J (2006) Spatiotemporal expression of zebrafish keratin 18 during early embryogenesis and the establishment of a keratin 18:RFP transgenic line. Gene Expr Patterns 6: 335–339.
63. de Oliveira S , Reyes-Aldasoro C C , Candel S , Renshaw S A , Mulero V , et al. (2013) Cxcl8 (IL-8) mediates neutrophil recruitment and behavior in the zebrafish inflammatory response. J Immunol 190: 4349–4359.
64. Pfaffl M W (2001) A new mathematical model for relative quantification in real-time RT-PCR. Nucleic Acids Res 29: e45.
65. Inoue D , Wittbrodt J (2011) One for all–a highly efficient and versatile method for fluorescent immunostaining in fish embryos. PLoS One 6: e19713.